

Aeolian transportation mechanics and mass movement of surficial beach sands – a case study on Bendi-Baruva Mineral Sand Deposit, Srikakulam District, Andhra Pradesh

Souradeep Mukherjee* and A.Yugandhara Rao

Atomic Minerals Directorate for Exploration and Research

*HomiBhabha National Institute

souradeepm.amd@gov.in

Abstract

Surficial sediment transportation studies carried out in the beach zone of Bendi-Baruva mineral sand deposit show that sand grains are transported by wind (saltation and suspension) beyond the high water line. The sand population of the study area contains heavy mineral sands (~20%) like ilmenite, garnet and sillimanite which covers 95% of the heavy mineral distribution with subordinate amounts of monazite, rutile, and zircon whereas light mineral sands (~80%) contain mostly quartz. Due to the sorted nature of these beach and dune sands the whole spectra falls within a specific range of grain size which shows a bi-modal distribution, primary mode at 0.025cm and secondary at 0.015cm. Due to this variation in density and grain size, mass of these sand particles vary resulting in differential transportation in any energy regime. In the study area, on the beach near the frontal dunes, surficial concentration of garnet grains are observed in patches having an average thickness 0.2cm i.e. around ten times of the dominant grain diameter. This surficial enrichment of garnet grains resting on a semi-uniform sand surface is the result of differential transportation of the dominant mineral grains. As more than 80% of the grain size population show a dominant grain size of 0.025cm, the wind flow parameters for the whole population is standardized with mean grain diameter (D) of 0.025cm. Mass of dominant individual minerals arrived from the grain counting technique was tallied with the theoretical mass considering spherical shape of the grains indicates a difference of mass to be within 5%. For ease of calculation and generalization the grains were considered to be spherical and their theoretical masses were taken into consideration in calculations. Considering the whole spectra of mineralogical distribution, a theoretical mass group distribution for dominant different minerals of different dominant grain sizes were formulated and total six mass groups were identified. Because quartz (~80%), ilmenite, sillimanite and garnet (together ~20%) are the most abundant, their positions were identified specifically in the theoretical mass groups and only these are considered for further discussion. To analyse wind velocity and pressure at different heights from the surface, a sediment trap was fabricated using piezo-electric sensors. A tail was attached to orient the device parallel to the wind flow so that the piezo surfaces always face the wind flow at 90° angle. The device records pressure data and converts those into voltage. Using the velocity data, macroscopic physical quantities of aeolian transportation were calculated for the study area, which empirically show the effect of mass in differential transportation of the dominant minerals that gives rise to these surficial garnet patches.

Introduction

In the beach zone, beyond high water line, transportation of sand grains is driven by wind. This dynamics of transportation is aided by sea-breeze and land-breeze in a daily manner which results in transportation of sands that are less in mass, leaving heavy mass behind. Mass of individual sand grains depends upon density and grain size (~volume). Product of these two physical properties generates a mass distribution in the area which reacts to wind flow differently causing a differential transportation. Surface creeping, saltation and suspension are the fundamental modes of aeolian transportation. Of these, saltation is the dominant one that covers up to 70% of the total mass movement (Bagnold, 1941; Shao, 2009). Again the initiation of surface creep and suspension is primordially caused by impact of the particles in saltation (Anderson et al., 1991a; Bagnold, 1941; Kok and Renno, 2009). So, the main transportation mode is governed and guided by the amount of saltation in a population of sand. Saltation is a response to fluid forces working on sediment-air

interface zone whenever shear velocities exceed a certain threshold (Bagnold, 1941). This transportation of grains occurs within the sediment-air interface where atmospheric parameters (e.g. wind speed, temperature and aerosol concentration) vary rapidly with height from the sediment surface, and turbulence is predominantly generated by wind shear (Shao, 2009). The relationship of wind speed with increasing height creates three types of wind profiles (parabolic, linear and hyperbolic / logarithmic). For the case at hand, this relationship is a logarithmic one, where the surface layer has the highest shear velocity (so the highest drag force) which drives the main transportation mechanism (Shao, 2009). This is why a daytime wind profile (a logarithmic one) dominates transportation of materials and most of the erosion and transportation occurs during the day (Shao, 2009). Theories have been propounded to identify and quantify macroscopic physical parameters such as wind velocity profile, transportation flux, rate of transport per unit width (Bagnold, 1941; Anderson et al., 1991; Kok and Renno, 2008). These physical parameters generate an overall idea on the distribution of energy and force on the mass groups which causes them to move. Sand grains

of different masses have different frictional threshold velocities (V_{*t}) which is a measure of force imparted on the particle when it is subjected to a fluid shear (Bagnold, 1941). This paper aims to empirically define the response of the dominant mass groups present in the area to the wind flow which gives rise to surficial concentration of garnet grains. To achieve that, in this paper dominant mass groups (mineral sands of different sizes and densities) were found out by weighing and daytime wind velocities were calculated using a piezoelectric sediment trap. Using these two parameters, mechanism of sand movement was theoretically derived and the response of each mass group (sand grains of different sizes and densities) to the wind imparted force was shown empirically.

Materials and Methods

To analyse the response of different groups of sand that vary in mass, a sediment trap was built using piezo-electric sensors (PZT-5H) to track the signature of transportation at different patches of heavy mineral concentration which recorded voltage output of the sensors. A tail was attached to the stand with ball bearing to orient the device parallel to the wind flow so that the piezo surfaces always face the wind flow at a 90° angle. The device records pressure data and converts those into voltage. The set-up was done following a typical component flowchart of any recording equipment i.e. sensor – amplifier – processor – recorder. The circuit diagram is shown in the figure 5. In this case piezo-electric chips (PZT-5H) were used as input sensors, LM-358 Op-Amps were used as amplifiers, Doit ESP-32 as microprocessors and a laptop was used as a recorder. The sediment trap is built by mounting Piezo-electric chips (sensors) on a PVC pipe (stand) with a cardboard sail (Tail) attached to it vertically. This whole arrangement is put on a stand using ball-bearings which allows height (levels) of the sensors to fix following the log law of the wind. From the output voltage the force imparted by the wind was calculated at different levels which further were used to calculate transportation dynamics of the dominant sand grains present in the area.

Dominant mass groups

The dominant surficial mineralogy of Bendi-Baruva mineral sand deposit, India was established by collecting of sand samples up to 1.5m depth at five different profiles 5 km apart with a grid of (5000m X 100m). The individual samples were analysed to draw an idea on the macro-component distribution, which shows that in light minerals (quartz) and total heavy minerals (THM) which together covers the whole sand population (Figure 1) which is dominated by quartz, ilmenite, garnet and sillimanite (around 95% of raw sand distribution). Grain size distribution of individual heavy minerals were formulated by physical separation techniques (bromoform separation as well as electro-magnetic separation) and sieving. The grain size

distribution for raw sand (i.e., sand without slime and shell content) and THM show a primary dominant mode of raw sand at 250 micron so the dominant sand diameter is taken to be of 0.025cm but contrastingly the heavy minerals have a primary dominant grain size at 150 micron. In figure 2, distribution of individual heavy minerals is shown. It is also seen that in these four dominant minerals (quartz, ilmenite, sillimanite, garnet), the grains occur in specific dominant grain sizes. The dominant sizes were selected as it covers more than 95% of the total grain size distribution and have the highest influence on grain transportation. To cover the whole population, calculation of theoretical mass of individual mineral grains were done considering sphere of equivalent diameter using the following formula (Bagnold, 1941):

$$m_s = \frac{\pi}{6} \sigma_s d^3 \quad (1)$$

where, m_s is the mass of the sand grain, σ_s is the density and d is the grain diameter.

Data for all of the dominant mineral groups were generated according to this equation to briefly identify the mass groups present in the area. Mass of each mineral pertaining to different sizes indicates that there exist small ranges where few values cluster (Fig. 3). This is compared with the dominant mineral mass groups to identify in which group it falls. In reality as the grains vary in shape and sizes, the mass also varies from the ideal calculated value. To check how closely it matches the theoretical mass, pure fraction of individual dominant heavy mineral grains of different dominant sizes (total 7) were measured by weighing a small sample and calculating total numbers of grain present in it, with the help of an optical microscope and dividing these two parameters (Fig.4). A comparative study in table 1 shows the percentage of error in mass calculation for these dominant sand grains and it is found to be less than 5%. Thus, equivalent spherical grains were considered for fluid dynamic studies to generate a very good approximation of natural events. Quartz is the dominant light mineral. For quartz grains, the theoretical values were taken. The whole population have six dominant mass groups (Fig.3) and the dominant ones are a small subset of those (Fig.4)

Calculation of wind velocity

Aeolian sand transport is a response to fluid forces within the near boundary of the surface whenever shear velocities exceed a certain threshold shear velocity (v_{*t}) (Bagnold, 1941, Poortinga, 2015). As the sediments behave differently to wind flow because of their mass, shape, co-efficient of friction, etc. the large scale structures and gradation in sediment distribution forms (Bagnold, 1941). For incompressible fluid flow, Navier-Stokes equation is used to determine turbulence, a chaotic eddying motion of a fluid with rapid variation in pressure and velocity in space and time which is a typical characteristic of wind flow and has been associated with the initiation of sediments movement

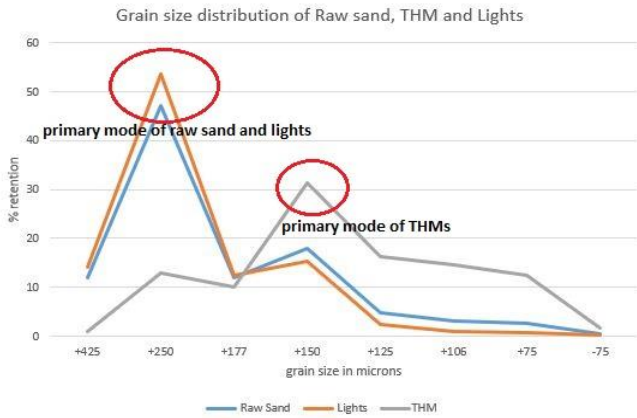


Fig.1. Grain size distribution of raw sand, THM and Light Minerals

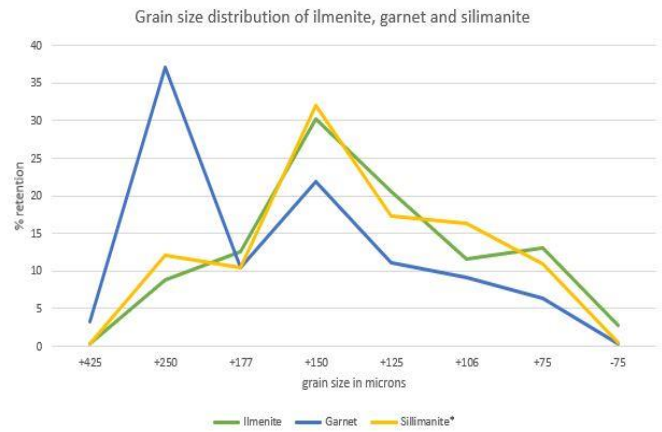


Fig.2. Grain size distribution of individual Heavy minerals

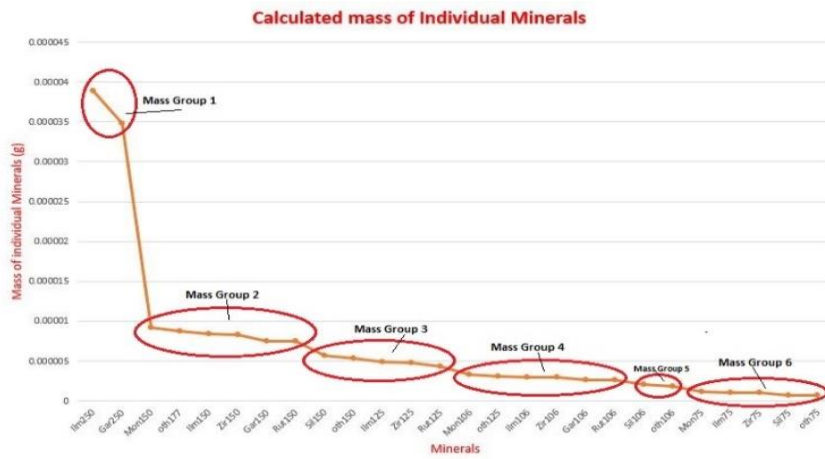


Fig.3. Calculated mass of individual minerals

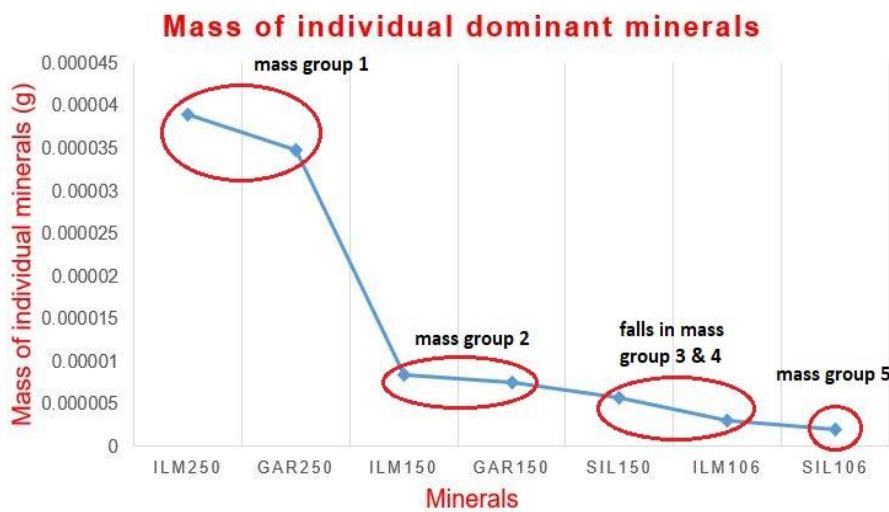


Fig.4. Mass of individual dominant minerals

(Walker, 2003). The dimensionless Reynolds Number (Reynolds, 1883, Bagnold, 1941) is derived from it and has an expression of:

$$R_e = \frac{\rho l v_r}{\eta} = \frac{V_* d}{\nu} \quad (2)$$

For the case at hand, a PZT-5H has a value of g_{33} of 20 (10^{-3} V-m/N), thickness of 0.5mm, and a diameter of 25mm. As the processing is done by a do it ESP-32 micro-processor which operated between 0-5

Minerals	Density (g/cm ³)	Size (cm)	measured mass total	no of grains	individual mass	calculated volume	calculated mass	error %
Ilm250	4.75	0.025	0.0063	160	0.000039375	8.1813E-06	3.88608E-05	1.32
Gar250	4.25	0.025	0.0044	125	0.0000352	8.1823E-06	3.47702E-05	1.23
Ilm150	4.75	0.015	0.0037	425	8.70588E-06	1.7615E-06	8.39394E-06	3.71
Gar150	4.25	0.015	0.0029	371	7.81671E-06	1.7615E-06	7.51037E-06	4.07
Sil150	3.23	0.015	0.0029	493	5.88235E-06	1.7615E-06	5.70788E-06	3.05
Ilm106	4.75	0.0106	0.0028	921	3.04017E-06	6.2314E-07	2.96217E-06	2.63
Sil106	3.23	0.0106	0.0018	878	2.05011E-06	6.2614E-07	2.01427E-06	1.7

For particle size range (r) of (0.001-0.1cm), relative velocity (v_r) of (10-2000 cm/s), R_e falls in a range of 10^2 - 10^3 which is a fuzzy area for velocity-resistance relation (Bagnold, 1941). Again wind flow imparts force on any surface it acts on, the force can be divided in two components, 1) at right angle to the surface (equation 3) and parallel to the surface (equation 4)(Bagnold, 1941).

$$p = \frac{1}{2} \rho v^2 \quad (3)$$

$$\tau' = \rho V_*^2 \quad (4)$$

where, p is force/unit area acting perpendicular to a surface, ρ is density of fluid, v is fluid velocity, τ' is the drag force and V_* is drag velocity. Clearly, V_* is not the speed of the flow but simply another expression for the momentum flux at the surface. As V_* is a convenient description of the force exerted on the surface by wind shear, it emerges as one of the most important quantities in wind-erosion studies (Shao, 2009). For this case, to calculate wind velocity in different levels and its signature on transportation, a sediment trap using piezo-electric sensor was used where piezo surfaces face the wind flow at right angle. A piezo-electric transducer generates voltage from imparted pressure (Platt, S. et al, 2005). For this study a low power PZT-5H chip was used as input sensor for the sediment trap. When wind hits the piezo surface at a right angle it imparts pressure on the piezo chip which in turn generates a static voltage. The equation for static voltage generation for a piezo-electric transducer is given below:

$$V = \frac{g_{33} F_3 h}{\pi r^2} \quad (5)$$

where static voltage V can be calculated from piezo-electric voltage constant g_{33} , force acted on the surface F_3 , thickness of the chip h and radius r. So the Force can be calculated by modifying the equation (5):

$$F_3 = \frac{\pi r^2 V}{g_{33} h} \quad (6)$$

Volts, amplification is selected on the basis of trial and error and finally set to be 50000. In this range the voltage output of the imparted pressure works properly. The pressure is calculated by dividing F_3 with the cross-sectional area (i.e. 4.908 cm²). Now, the pressure imparted can be transformed to generate velocity data using equation (3) and this generates mass distribution in the area. The Circuit diagram of the set-up is shown in (Fig.5) and the picture of the trap is shown in (Fig.6a and 6b). The data acquisition (sampling time and repeatability) details are given in table 2. As the sampling frequency of this type of processors is very high, only the averaged value of static voltage in different levels is given in Table 3.

Wind speed vs height has been plotted and the relationship of these two parameters is exponential. The result shows a very good co-relation with a R^2 value of 0.96 (Fig.7). This type of wind profile is stated as unstable as it shows a more sheer velocity near the boundary layer which dominantly drives erosion (Shao, 2009). The wind load is also calculated from the wind velocity value by using the following expression (Bagnold, 1941):

$$F = A \cdot C_d \cdot P \quad (7)$$

where, F is the wind-load, A is the cross-sectional area of the piezo chips, drag-coefficient C_d and P is the calculated wind pressure. This wind load also follows the same trend when it is plotted against height.

Sediment transportation

When a sand particle moves through air, two fundamental forces have a negative impact on the flight of the particle i.e. downward force of gravity and air resistance in the direction opposite to the relative movement (Bagnold, 1941). The ratio of these two forces termed susceptibility (S). It is given by the following impression (Bagnold, 1941): $S = \frac{P}{mg}$ (8)

where, P is the force experienced by the particle horizontally which can be derived from the modification of equation (3) by introducing drag-coefficient C_d or c (in equation 9). C_d for smooth spherical grains travelling

through air is to be taken as 1.8 (Bagnold, 1941). The ‘m’ in the denominator is to be calculated using equation (1) which gives the following expression for susceptibility

Table.2 Data acquisition details for three selected patches (each has been repeated for 5 times)

Acquisition	Lat	Long	Date	Time	Tail direction	Avg Direction
1	18°45'1.82"N	84°30'8.96"E	8th April	11:00	336	
2	18°45'1.82"N	84°30'8.96"E	8th April	11:05	342	
3	18°45'1.82"N	84°30'8.96"E	8th April	11:10	329	332.8
4	18°45'1.82"N	84°30'8.96"E	8th April	11:15	330	
5	18°45'1.82"N	84°30'8.96"E	8th April	11:20	327	
6	18°43'5.21"N	84°28'19.27"E	12th April	09:00	319	
7	18°43'5.21"N	84°28'19.27"E	12th April	09:05	325	
8	18°43'5.21"N	84°28'19.27"E	12th April	09:10	320	319.6
9	18°43'5.21"N	84°28'19.27"E	12th April	09:15	312	
10	18°43'5.21"N	84°28'19.27"E	12th April	09:20	322	
11	18°47'17.69"N	84°32'55.06"E	20th April	11:00	349	
12	18°47'17.69"N	84°32'55.06"E	20th April	11:05	356	
13	18°47'17.69"N	84°32'55.06"E	20th April	11:10	348	351.4
14	18°47'17.69"N	84°32'55.06"E	20th April	11:15	356	
15	18°47'17.69"N	84°32'55.06"E	20th April	11:20	348	

Table.3 Calculation of wind speed from piezo data

Sensor no	channel no	Pin No	Height (cm)	Sampling frequency	Amplification	Area (sq.cm)	Voltage	Pressure (dyne/sq.cm)	Speed (cm/s)	Wind load (gm)
1	COM5	A3	5	9600	50000	4.9085	1.4694	29.389	219.5	29.534
2	COM5	A6	12	9600	50000	4.9085	1.6805	33.612	234.7	33.778
3	COM5	A7	19	9600	50000	4.9085	2.034	40.682	258.2	40.882
4	COM5	A4	26	9600	50000	4.9085	2.3101	46.203	275.2	46.431
5	COM5	A5	50	9600	50000	4.9085	2.9559	59.121	311.3	59.412
6	COM5	A8	100	9600	50000	4.9085	3.534	70.682	340.4	71.030

(Bagnold, 1941): $S = \frac{3\rho v^2 c}{4\sigma_s g d}$ (9)

values for all the dominant grains were calculated and plotted against different wind speeds at different heights. This generates a plot (Fig.8) which defines how the grains will be susceptible to transportation and if their mass and grain size play any role on it. It can be clearly seen from the plot that the susceptibility values show an exponentially decreasing trend which is quite similar to the mass group clusters. This proves the bearing of mass on transportation where silimanite₁₀₆ is more prone to travel than Ilmenite₂₅₀ mathematically which will be clearly seen when the forces for transportation will be calculated subsequently. The same mass groups show

similar clustering in the susceptibility values. But for grain movement and saltation, drag force drives the whole mechanism. To tract the grain movement and their motion path, calculation of drag force is essential, and it was calculated graphically from wind speed data. Drag force is defined by equation (4) where V^* value is required. This V^* is called as drag velocity or velocity gradient which is defined by the slope of the tangent at a wind speed vs levels (in logarithmic scale) (Fig.9) diagram (Bagnold, 1941). So V^* is proportional to the tan value of the angle made by the tangent with the y-axis in the figure 9.

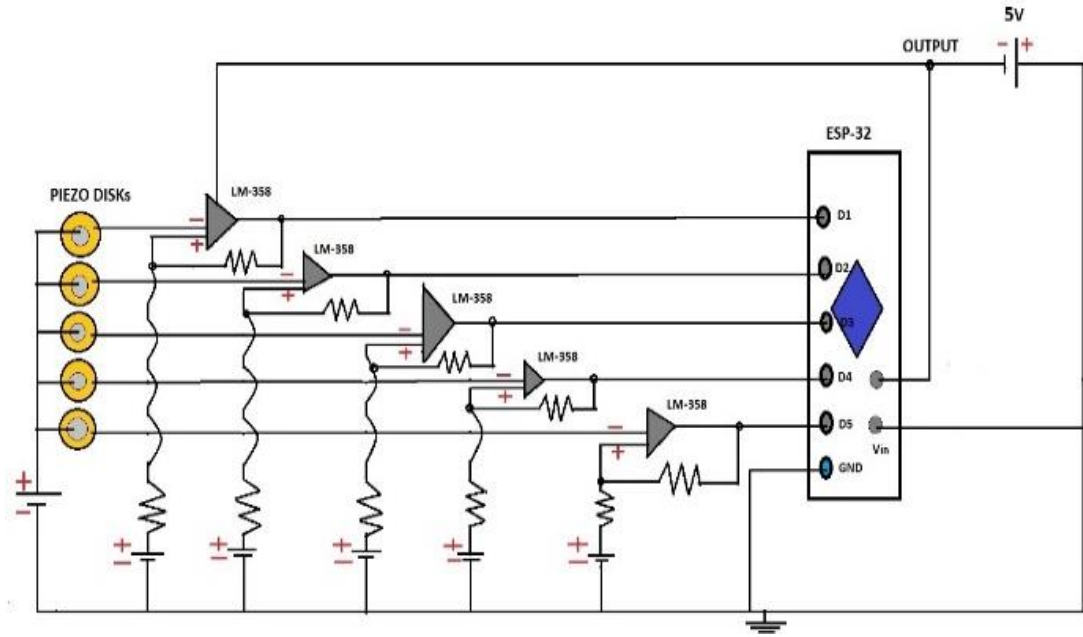


Fig.5. The Circuit diagram of Piezo-opamp-esp32 setup (only 5 piezo sensors are shown for better representation)

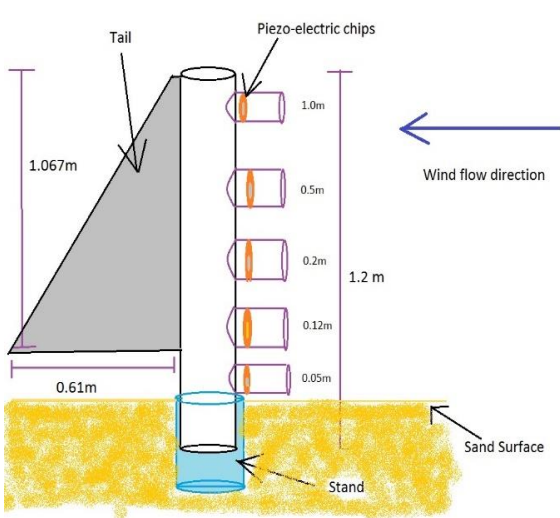


Fig.6a. The Sediment trap at work (only 5 piezo)

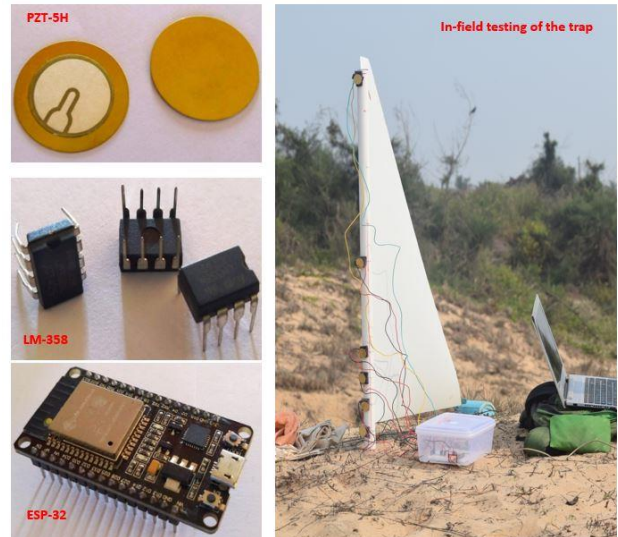


Fig.6b. The Sediment trap at work

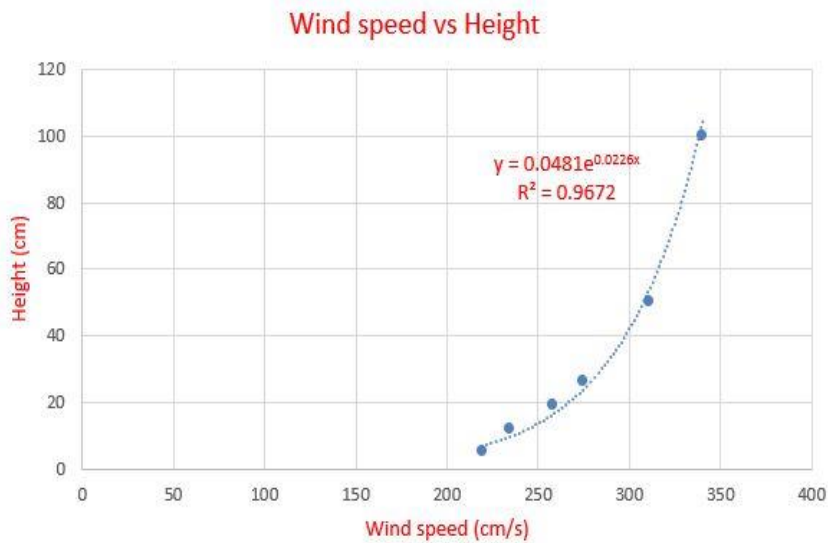


Fig.7. Wind speed vs height from the ground surface

$$V_* = \frac{AC}{CO'} \tan\theta \quad (10)$$

where $\theta = 64^\circ$, $AC = (V_{100} - V_{12})$, $OC' = \log(z) - \log(k')$. Here for the calculation k' is taken as 12cm which is the height of the second sensor, and thus using equation (9), V_* was calculated and found to be 125.97cm/s. Roughness length (k) was calculated from the y axis intercept of the tangent and has a value of 0.47cm which defines the zero velocity height. So any saltation will take place above that level. Now the effect of this drag force (τ') on the sediments causes them to move. The drag force was calculated using equation (4), which is found to be of 19.36 dyne. To track the response of the encountered mass groups to the wind flow, another two important parameters (Frictional threshold) were calculated- 1) Fluid threshold or static threshold and 2) impact threshold or dynamic threshold. Fluid threshold defines the minimum velocity of the fluid to act on a particle causing it to move. Fluid threshold can be calculated using the equation (Shao and Lu, 2000):

$$V_{*t} = A_s \sqrt{\frac{(\sigma_s - \rho)}{\rho} gd + \frac{\gamma}{\rho d}} \quad (11)$$

where $\frac{\gamma}{\rho d}$ is added to modify the equation for fine particles ($d < 0.008$ cm), but as our domain of work resides in the comparatively coarse grains (0.025cm), the normal Bagnold equation is used (Bagnold, 1941):

$$V_{*t} = A_B \sqrt{\frac{(\sigma_s - \rho)}{\rho} gd} \quad (12)$$

$$V_{*t} = A_B \tan\theta \sqrt{\frac{(\sigma_s - \rho)}{\rho} gd \log\left(\frac{z}{k'}\right)} \quad (13)$$

where A_s (equation 11) and A_B (equation 12, 13) are constants derived by Shao and Bagnold. Equation (13) gives V_{*t} at different levels. Using this equation static or fluid threshold for the dominant mass groups were identified (Fig.10). V_{*t} values for 1cm, 5cm, 12cm, 9cm, 26cm, 50cm, 1m are plotted serially and two types of trend were identified. The vertical curves connect the same mineral grains of different sizes and the horizontal curves connect the mass groups having similar fluid threshold values. These horizontal curves connecting different mineral grains of different sizes suggest the same range of portability for a group of minerals subjected to a fixed value of wind velocity. As with increasing height wind speed increases along with potential energy of particles, it requires more threshold velocity for transportation. Now 1 cm level is the value of k' for dune sands (Bagnold, 1941), saltation takes place just above this height. Thus the dynamic or impact threshold was calculated for 1cm height using the following equation (Bagnold, 1941):

$$V_t = A \tan\theta \sqrt{\frac{(\sigma_s - \rho)}{\rho} gd \log\left(\frac{k'}{k}\right)} \quad (14)$$

For this study, A is taken as 0.08, K' is 1 cm and roughness constant k was calculated to be 0.47cm which converts the expression to:

$$V_t = 0.0537 \sqrt{\frac{(\sigma_s - \rho)}{\rho} gd} \quad (15)$$

Impact threshold was calculated for the dominant mass groups using equation (15), details of these threshold values are given in table 3. From figure 11 an idea can be drawn on how V_{*t} varies for different mineral grains. It is clearly seen that each mass group has a range of fluid thresholds, Sil_{106} having the least values. The less the values of V_{*t} , more easily it will get transported because the wind flow imparted pressure will get distributed among the least V_{*t} values (Bagnold, 1941). Figure 12 shows a plot of grain diameter in negative ϕ values with threshold velocities. As For Gar_{250} the cut off limit of grain movement (i.e. the lowest value for V_t) is found to be 15.708 cm/s, below that limit Gar_{250} is immovable. The mass groups having higher values were spotted for both the V_{*t} and V_t values as they can generate collision imparted pressure on Gar_{250} for which it will move. Grains like Ilm_{250} , Ilm_{150} , Qtz_{250} and Gar_{150} can make the Gar_{250} grain move by collision, as their V_{*t} values fall close to V_t of Gar_{250} . So it can be inferred from the values that before a Gar_{250} grain can move, a lot of other dominant minerals have already experienced Aeolian transportation (Fig.13). It is also seen from the figure 13 that the dominant mass groups of the study area fall in the saltation range. A typical uniform saltation mechanism in this domain of flow, is governed by combination of three dominant force forces - 1) Drag force on particles (F_D) which causes particles to move in the viscous layer or flow and 2) aerodynamic lift (F_L) caused by the velocity gradient which gives the lift off angle to the saltating particles and weight of the particle. So the forces to move these encountered group of particles individually (ignoring Magnus force and electric force), are calculated by these equations (Shao, 2009):

$$F_S = F_D + F_L - F_g \quad (16)$$

Individual drag and lift were calculated using the following equations (Shao, 2009):

$$F_D = \frac{1}{2} C_d \rho A v_r V_r \quad (17)$$

$$F_L = \frac{1}{2} C_{ld} \rho A (\nabla V)^2 d \quad (18)$$

For sediment transportation by saltation, the frictional threshold velocity for each mineral was considered which modifies the $v_r V_r$ values as V_{*t}^2 and ∇V defines the gradient of v for the considered particle to move. It is seen from experimental data, $C_1 = 0.85 C_D$. So the combined force required for saltation of sand grains is calculated from the following equation:

$$F_S = \frac{1}{2} C_{ld} \rho A V_{*t}^2 d + \frac{1}{2} C_d \rho A - mg \quad (19)$$

This is the necessary equation to calculate force exerted on individual mineral grains which are subjected to saltation. The values of the different forces calculated are given in table.4.

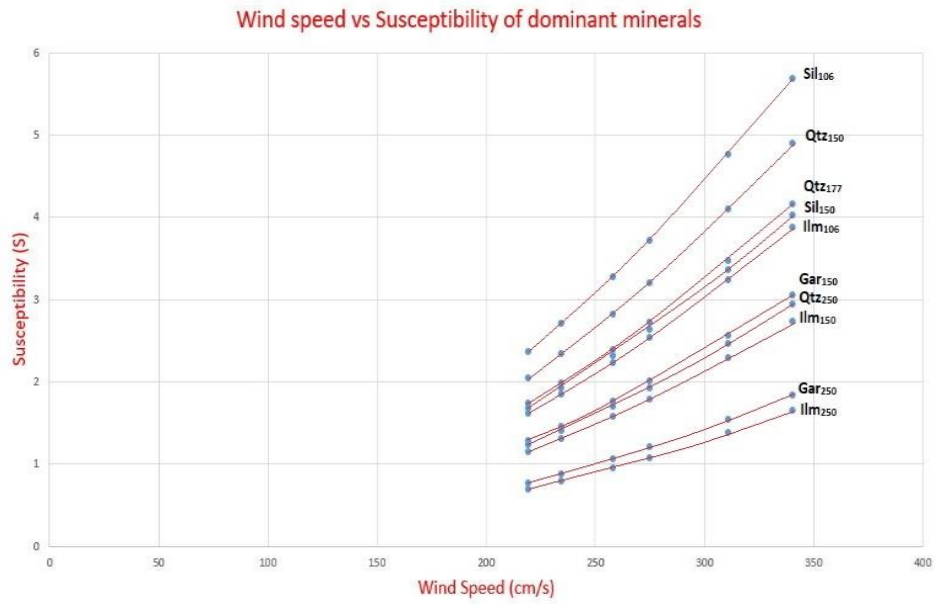


Fig.8. Wind speed vs Susceptibility

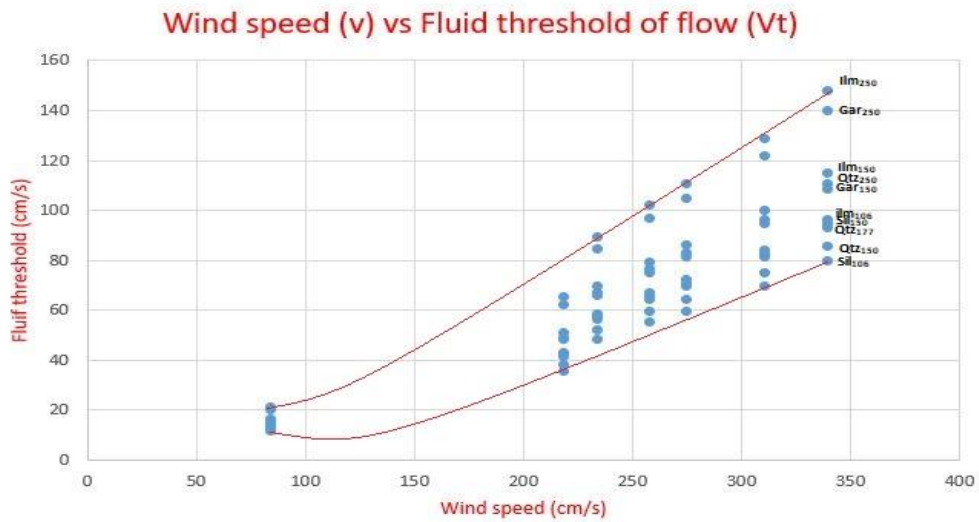


Fig.9. Calculation of V^* , K

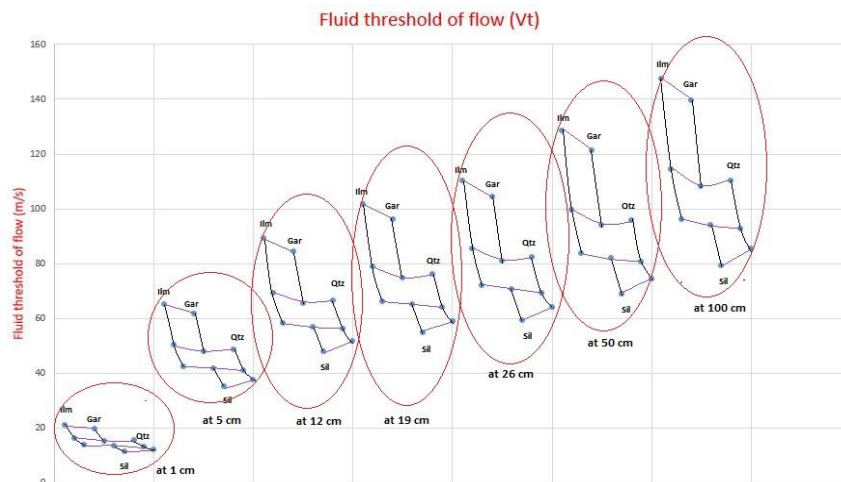


Fig.10. Fluid threshold (V_{*t}) of dominant mass groups in different heights

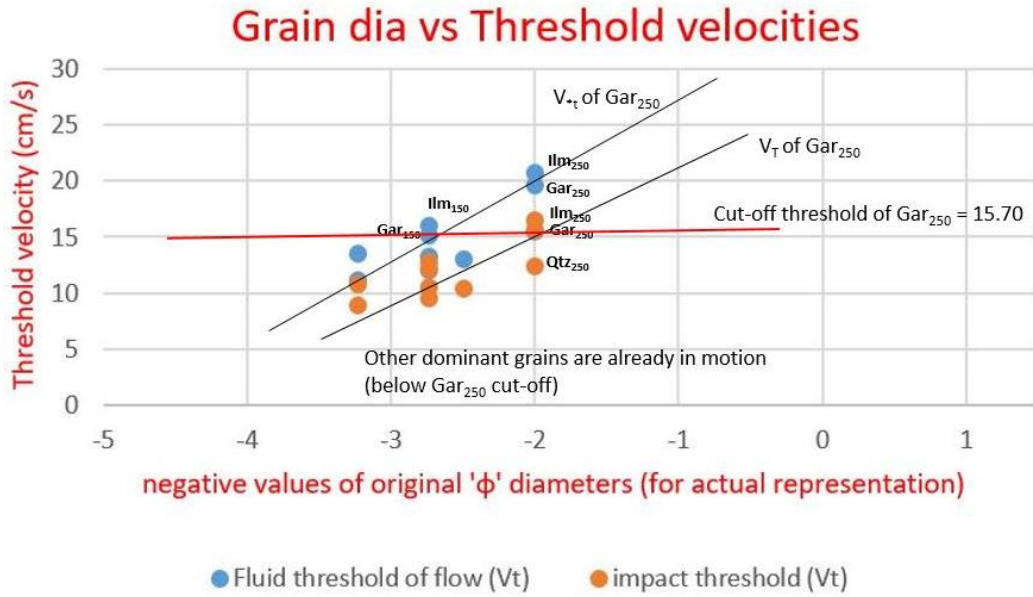


Fig.11. Wind speed vs Fluid threshold (V_{*t}) of dominant mass groups at different heights

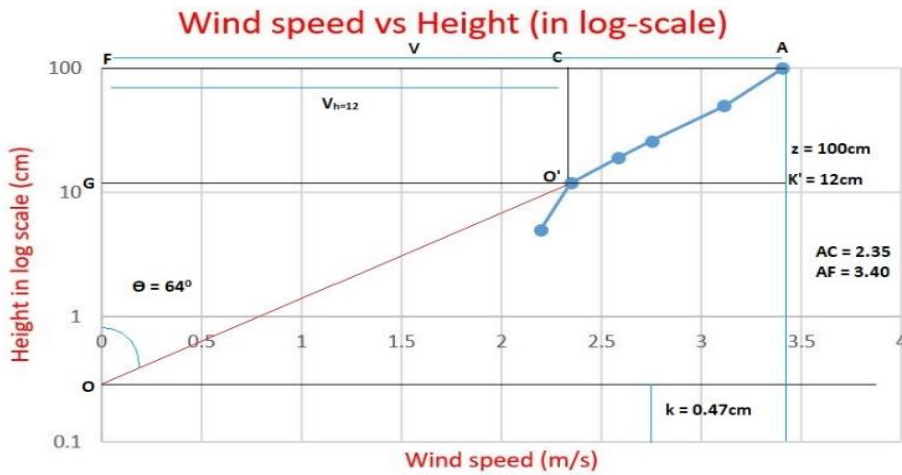


Fig.12. Grain dia vs threshold velocities (V_{*t} , V_t) of dominant mass groups at 1cm height

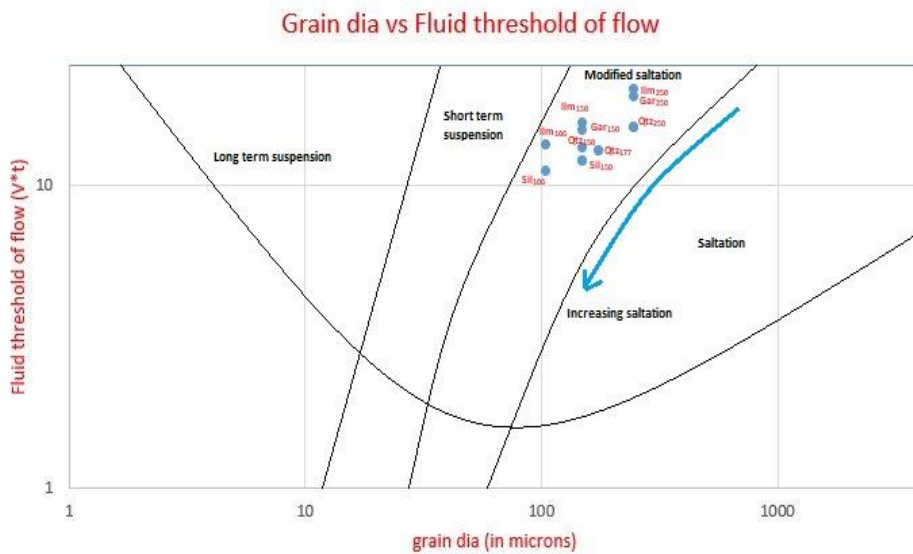


Fig.13. Frictional threshold (V_{*t}) of dominant groups plotted against grain diameter in log scale

Minerals	V*t	V _T	F _D	F _i	mg	Minimum force for saltation (F)	maximum number of transported grains
Ilm250	20.758	16.607	0.904	0.01921	0.038	0.885	22
Gar250	19.635	15.708	0.724	0.01538	0.034	0.705	27
Qtz250	15.503	12.403	0.281	0.00598	0.021	0.266	73
Ilm150	16.079	12.863	0.195	0.00249	0.008	0.19	102
Gar150	15.209	12.167	0.156	0.00199	0.007	0.151	128
Qtz177	13.045	10.436	0.1	0.0015	0.008	0.094	206
Sil150	13.259	10.607	0.09	0.00115	0.006	0.086	225
Ilm106	13.517	10.813	0.069	0.00062	0.003	0.067	289
Qtz150	12.009	9.607	0.061	0.00077	0.005	0.057	340
Sil106	11.146	8.916	0.032	0.00029	0.002	0.03	645

It is clearly seen that, in the given energy regime a single grain of Ilm₂₅₀ requires the highest amount of force to get transported (0.885 dyne) whereas a grain of Sil₁₀₆ requires the least force (0.03 dyne). Drag force per unit width calculated from equation (4) were found to be of 19.36 dyne. Hypothetically for a uniform distribution of monomineralic sand, this force will be distributed over unit width among the grains. So, shear force in unit time and unit width can transport maximum numbers of sand grains which is calculated by dividing the total imparted force by minimum transportation force. It can now be seen that, for a constant value of V* = 125.97 cm/s, only 27Gar₂₅₀ grains can get transported in unit time compared to 646 grains of Sil₁₀₆. Another important relationship arises when different susceptibility values were plotted against F_s. These two parameters have a logarithmic relationship:

$$S = -A_1 \ln(F_s) + B_1 \quad (20)$$

As susceptibility is the independent variable here, the equation (20) changes to this exponential form:

$$F_s = A_2 e^{-B_2 S} \quad (21)$$

where, A₁, B₁, A₂, B₂ are constants, A₁=0.482 and B₁=0.5198, and A₂=2.5907, B₂ = 1.988 measured at the top limit of the saltation layer, i.e. at 5cm. This shows how the encountered mass groups of the area behave differently when they are subjected to a wind flow. Gar₂₅₀ and Ilm₂₅₀ has the highest requirement of force thus has a low susceptibility. These two mineral groups exist separately where rest of the values cluster, this comparative mobility of higher susceptible grains separate them from Gar₂₅₀ and Ilm₂₅₀ making these two relatively left out in transportation causing a local enrichment of these mineral grains in the encountered energy domain. Due to the nature of the source, Ilmenite sand occurs mostly at 0.015cm diagenetically (primary mode at +150 micron), making Gar₂₅₀ dominating the local residue enrichment patches.

Observations and Discussion

Bendi-Baruva mineral sand deposit of North Srikakulam, shows a typical beach and dune sand regime which is subjected to daily wind flow with average velocity of 3m/s. Wind velocity of this value falls between a domain where R_e has a value (R_e= 38.11) of 10⁻²<R_e<10³ which is a fuzzy domain between Stoke's region (<10⁻²) and high turbulent region where C_d is constant (>10³). For this domain, R_e reduces with increasing C_d for a fixed grain size. The Flux-gradient relationship of atmospheric boundary layer shows an unstable wind flow profile during day time where drag force near the ground surface is maximum thus transportation and erosion takes place mostly during daytime. Hence the measurements were made during the day time. The mineralogical distribution in the area shows dominance of four minerals (Ilmenite, Garnet, Sillimanite, and Quartz) of specific grain sizes. The overall grain size distribution of the raw sand has an average diameter of 0.025cm, and 0.015cm for the most of heavy minerals (except Garnet). The wind flow in the beach zone imparts drag force on the particles which causes transportation of these particles. Different particles behaves differently to the imparted drag force (τ=19.36 dyne) because of their mass, volume, grain size. Partition of force on sand grains is guided by the velocity gradient (V*) of the flow and frictional threshold velocities (V*_t) of the particle which is an impression of minimum force for transportation. V*_t values of dominant mass groups fall in the region of saltation when it is plotted against grain diameter, which proves the dominant mode of transportation is saltation. The maximum height for saltation for a standard aeolian transportation process in dune sands is about 5cm so V*_t values were calculated at this height where drag force is maximum for saltation. This sets the upper limit of exerted force for saltation. Ilm₂₅₀ and Gar₂₅₀ having the highest V*_t requires maximum amount of drag force for getting transported. Individual minimum force required for saltation using equation (19) also gives out an identical picture. Susceptibility (S) which is a measure of

ease of lateral movement of particles in a flow, when plotted against the minimum force required for saltation, shows an exponential decrease in susceptibility value with increasing requirement of saltation force. This clearly separates out Gar₂₅₀ grains from the other dominant mineral groups as relatively immobile one (Ilm₂₅₀ is not considered as its primary mode of grain size is 0.015cm so Ilm₁₅₀ is the dominant grain size for Ilmenite followed by its finer fractions). Due to this fraction of relative immobility in this energy domain Gar₂₅₀ is relatively left out during transportation causing a local surficial enrichment of these grains which is visible as patches on the beach zone. This signature is more prominent at Srikurmam, 70km southward of Bendi-Baruva which shows one of the highest surficial enrichment of coarse garnet grains in India.

Acknowledgement

I express my sincere gratitude to the Director, Atomic Minerals Directorate for Exploration and Research and Head, Beach Sand and Off-shore Investigation group, for their constant encouragement, permission and support to make this work a successful completion.

Funding: No funding.

Conflict of interest: The authors do not have any conflict of interest.

References

- Anderson R S, Haff P. K. (1988). Simulation of aeolian saltation. *Science*, 241(4867): 820–823.
- Anderson R. ., Sorensen M., Willetts B. B. A review of recent progress in our understanding of aeolian sediment transport. *ActaMechSuppl*, 1991, 1: 1–20.
- Bagnold R. A. (1941). *The Physics of Blown Sand and Desert Dunes*. London: Methuen
- Kok J. F., Renno N. O. (2009). A comprehensive numerical model of steady state saltation (COMSALT). *Journal of Geophysical Research: Atmospheres*, 114(D17): D17204.
- Platt, S. R., Farritor, S. M., and Haider, H. (2005). On Low-frequency electric power generation with PZT ceramics. *IEEE/ASME Transactions on Mechatronics*, 10(2), 240-252.
- Poortinga. Ate. (2015). *Beach Sand Dynamics: measurements, models and scales Wageningen: Wageningen University*.
- Reynolds, O. (1883). An experimental Investigation of the Circumstances Which Determine Whether the Motion of Water Shall Be Direct or Sinuous, and of the Law of Resistance in Parallel Channels, *Philosophical Transactions of the Royal Society of London*, Vol. 174, pp. 935-982
- Shao, Y., Lu, H., (2000). A simple expression for wind erosion threshold friction velocity. *J. Geophys. Res.* 105, 22437–22443.
- Shao. Y. (2009). *Physics and Modelling of Wind Erosion*. Germany.
- Walker, I.J. and W.G. Nickling. (2003). Simulation and measurement of surface shear stress over isolated and closely spaced transverse dunes in a wind tunnel. *Earth Surface Processes and Landforms* 28(10), 1111–1124.
- Wyngaard JC (1990) Scalar fluxes in the planetary boundary layer –theory, modelling and measurement. *Boundary-Layer Meteorol*50: 49–75
- Yamada T., Mellor G. L. (1975) A simulation of the Wangaraatmospheric boundary layer data. *J AtmosSci* 32: 2309–2329.

Received: 23rd June, 2020

Revised accepted: 6th October, 2021